1Pa-53

Proceedings of Symposium on Ultrasonic Electronics, Vol. 31 (2010) pp. 121-122
6-8 December, 2010

Determination of Optimal Cardiac Phase for Automated Identification of the Heart Wall Region Using Multiple Features of RF Echoes

RFエコーの複数の特徴量を用いた心臓壁領域同定の自動化における最適心時相の決定

Hiroki Takahashi[1‡], Hideyuki Hasegawa[1,2] and Hiroshi Kanai[2,1]
([1]Grad. School of Biomed. Eng., Tohoku Univ.; [2]Grad. School of Eng., Tohoku Univ.)
高橋広樹[1‡]，長谷川英之[1,2]，金井　浩[2,1] ([1]東北大院 医工; [2]東北大院 工)

1. Introduction

Various valuable evaluation methods of cardiac function based on echocardiography, such like ultrasonic Doppler technique, have been researched, for example, evaluation of 2-D cardiac wall motion by speckle tracking method[1,2] and measurement of propagation of vibration caused by electrical excitation in the human heart[3]. In most cases, the heart wall region, which is the object to be analyzed, is currently identified manually for evaluation of cardiac functions. However, for elimination of the operator dependence and improvement of ease of analysis, automated identification of the heart wall is essential. By identifying the heart wall region on RF data at an initial frame, the heart wall at the following frames can be identified by tracking the heart wall motion using 1-D or 2-D tracking methods. In the present study, the heart wall region at an initial frame was identified automatically by classification using multiple features extracted from echo signals which are measured at a high frame rate. Furthermore, we investigated the optimal cardiac phase for classification by multiple features.

2. Feature Extraction

The magnitude-squared coherence (MSC) function[4], $|\gamma_{x,n}(f)|^2$ (at $f = 4.2$ MHz), at a depth x in the nth frame using complex spectra of echo signals in the tracked areas is used as the first feature.

Analytic signal $y_1(x; n)$ is obtained by applying the quadrature demodulation to RF signals $s_1(x; n)$. In this case, $s_1(x; n)$ was high-pass filtered using moving target indicator (MTI) filter due to reduction of clutter components mainly reflected from the ribs. Using analytic signal $y_1(x; n)$, the envelope $Env(x; n)$ of $s_1(x; n)$ is given by

$$Env(x;n)=10\log_{10}\left[\sum_{i=-M_d}^{M_d}\left|y_1(x+i\cdot\Delta x;n)\right|^2\right] \quad [\mathrm{dB}], \quad (1)$$

where Δx and M_d are the interval of sampled signal in the depth direction and the number of sampled points used for calculating envelope, respectively. The envelope is used as the second feature.

The phase shift due to axial motion of tissue is measured using the complex correlation technique. In this study, the axial velocity of tissue is evaluated by estimator based on correlation of analytic signals $y_2(x; n)$ of RF signals $s_2(x; n)$ in multiple frames. In this case, RF signals $s_2(x; n)$ was also high-pass filtered, however, the cutoff frequency of the filter used for $s_2(x; n)$ is higher than that for $s_1(x; n)$ due to reduction of multiple reflection components from heart wall. Complex correlation function, $R(x; n)$, is given by

$$R(x;n)=\sum_{i=-M_d}^{M_d}\frac{\sum_{k=-M_t}^{M_t}y_2^*(x+i\cdot\Delta x;n+k)\,y_2(x+i\cdot\Delta x;n+k+1)}{\sqrt{\sum_{k=-M_t}^{M_t}\left|y_2(x+i\cdot\Delta x;n+k)\right|^2}\sqrt{\sum_{k=-M_t}^{M_t}\left|y_2(x+i\cdot\Delta x;n+k+1)\right|^2}}, \quad (2)$$

where M_t is the number of frames used for calculation of the correlation function. The absolute value of the phase shift obtained by the estimator given by Eq. (2) is used as the third feature. In this study, to accurately differentiate the heart wall from the lumen using features based on the phase shift, RF echo signals were measured at a high frame rate using parallel beamforming (PBF) with plane wave transmission[5] for prevention of aliasing.

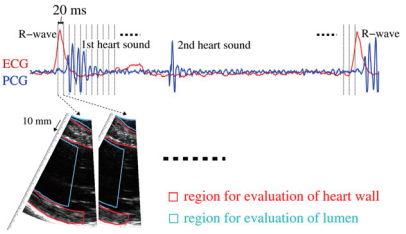

Fig. 1 Regions manually assigned for evaluation of separability between heart wall and lumen.

3. Determination of Optimal Cardiac Phase

As shown in **Fig. 1**, using RF data of the heart of a 23-year-old male at a high frame rate of 1010 Hz obtained by PBF, regions for evaluation of separability between heart wall and lumen were manually assigned. Using 3 features extracted as described above at each point in these regions, the criterion of class separability[6] J of feature vector is evaluated using prior probabilities $\{p_h\}$, mean

Email: h_taka@us.ecei.tohoku.ac.jp
(hasegawa, hkanai)@ecei.tohoku.ac.jp

vectors $\{\boldsymbol{\mu}_h\}$ and covariance matrixes $\{\boldsymbol{\Sigma}_h\}$ calculated for classes $\{\omega_h\}$ (lumen ($h = 0$) and heart wall ($h = 1$)) as follows:

$$J = \mathrm{tr}\left[\left(\sum_{h=0}^{1} p_h \boldsymbol{\Sigma}_h\right)^{-1}\left(\sum_{h=0}^{1} p_h (\boldsymbol{\mu}_h - \boldsymbol{\mu}_0)(\boldsymbol{\mu}_h - \boldsymbol{\mu}_0)^{\mathrm{T}}\right)\right], \quad (3)$$

where $\boldsymbol{\mu}_0$ and tr[・] are the mean vector of all entered feature vectors at the frame and sum of diagonal components, respectively. J shows the degree of separability between mean vectors of classes normalized by the sum of variances of feature vectors. **Figures 2**(a) and 2(b) show J obtained at the interval of 20 ms from the R-wave and velocities of interventricular septum (IVS) and left ventricular posterior wall (LVPW) estimated by phased tracking method[7]. Class separability is very low in the cardiac phases, when cardiac muscle is moving very slowly, such as slow filling phase, due to great reduction of backscatter components from heart wall by MTI filtering. On the other hand, class separability in the cardiac phases, when cardiac muscle is moving very fast, such as just after the time of R-wave[2], is also low due to degradation of separability of MSC. In cardiac phases, when blood flow velocity is high while myocardial velocity is not so high, such as during the transition from rapid filling phase to the slow filling phase, class separability is high. From these results, there are two conditions of cardiac phase for high class separability as follows:

[1] Myocardial velocity is not too low, but not so high.
[2] Blood flow velocity is high.

As described above, optimal cardiac phase for classification by above-mentioned features is during the transition from rapid filling phase to the slow filling phase, in addition, the ejection phase and atrial systole are also valid.

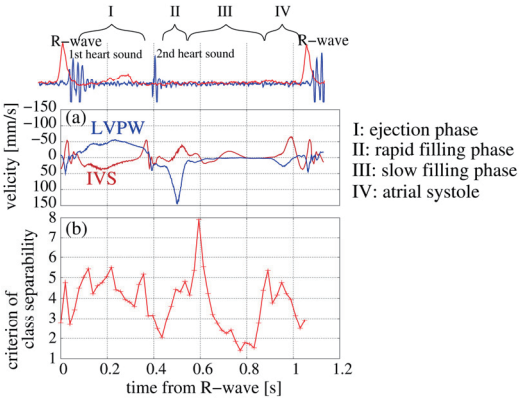

Fig. 2 (a) Spatial-mean velocity of IVS and LVPW estimated by phased tracking method. (b) Class separability given by Eq. (3).

4. Automated Identification of the Heart Wall

Figures 3(a) show a B-mode image and region-identified image, in which region identified using expectation-maximization (EM) algorithm[8] was colored. The initial parameters (supervising data) of EM algorithm were learned from manually assigned regions for heart wall and lumen, at a frame during the transition from the rapid filling phase to the slow filling phase. As shown in Fig. 3(a), heart wall region was accurately identified at the initial frame, and the identified regions were assigned for tracking positions of heart wall. Figures 3(b) and 3(c) show B-mode and region-identified images at the frames in two different cardiac phases, in which the heart wall region was identified by tracking the points classified as the heart wall region in Fig. 3(a).

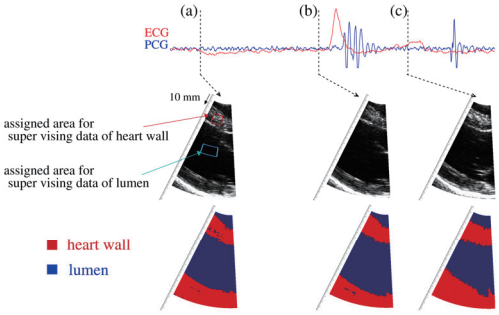

Fig. 3 (a) B-mode and region-identified images at the initial frame in optimal cardiac phase. B-mode and region-identified images obtained by tracking identified heart wall (b) during the period just before R-wave and (c) during ejection phase.

5. Conclusion

In this study, we proposed a method for automated identification of the heart wall region at multiple frames in a cardiac cycle using multiple features and the determined optimal cardiac phase for classification by proposed features. To apply the proposed method to ultrasonic images in various cardiac views, the optimal phase should be further investigated in the short axis and apical views.

References

1. J. D'hooge, et al: IEEE Trans. UFFC. **49** (2002) 281.
2. Y. Honjo, H. Hasegawa and H. Kanai: Jpn. J. Appl. Phys. 49 (2010) (in press).
3. H. Kanai: IEEE Trans. UFFC. **51** (2005) 1931.
4. T. Kinugawa, H. Hasegawa and H. Kanai: Jpn. J. Appl. Phys. **47** (2008) 4155.
5. H. Hasegawa and H. Kanai: IEEE Trans. UFFC. **55** (2008) 2626.
6. K. Fukunaga: Introduction to Statistical Pattern Recognition (2nd ed.) (Academic Press, Inc., CA, 1990).
7. H. Kanai, et al: IEEE Trans. UFFC. **43** (1996) 791.
8. A. P. Dempster, N. M. Laird and D. B. Rubin: J. R. Statist. Soc. Ser. B **39** (1977) 1.